Cytochrome P450 Mediated Aromatic Oxidation: A Theoretical Study

Kenneth Korzekwa,[†] William Trager,[†] Martin Gouterman,[†] Dale Spangler,[‡] and Gilda H. Loew*[‡]

Contribution from the Departments of Medicinal Chemistry and Chemistry, University of Washington, Seattle, Washington 98195, and the Life Sciences Division, SRI International, Menlo Park, California 94025. *Received July 17, 1984*

Abstract: Semiempirical molecular orbital calculations (MNDO) are used to model possible reaction pathways for cytochrome P450 catalyzed aromatic oxidation and to clarify the role of epoxide intermediates during phenol formation. Both biradical and protonated cationic pathways leading to epoxides, ketones, and phenols are characterized for a series of substituted benzenes and naphthalene. The calculated heats of formation and other thermodynamic properties of the geometry-optimized reactants, products, intermediates, and transition states give free energies of activation and the calculation of kinetic isotope effects. The results of this study indicate that biradical pathways show little or no substituent effects and the order of reaction rates is epoxide > ketone > phenol. The cationic pathways show marked substituent effects, and the order of reaction rates is reversed with phenol > ketone > epoxide. These results suggest that cationic as well as radical pathways may be involved in cytochrome P450 mediated aromatic oxidation.

Cytochromes P450 are a class of monooxygenase enzymes which are capable of a variety of oxidation reactions and show diverse substrate specificity. It is the primary enzyme complex involved in the metabolism of numerous xenobiotics; and, while usually producing a metabolite which can be more easily eliminated, it can also result in the formation of reactive intermediates which may lead to toxicities and/or carcinogenesis. For this reason, a great deal of research has been directed toward the elucidation of the mechanisms involved.

Arene oxides have been recognized as one of the toxic intermediates resulting from aromatic oxidation, with evidence provided by epoxide trapping experiments[1] and the isolation of naphthalene oxide from microsomal preparations.[2] Also, the amount of deuterium retained in the substrate due to the "NIH shift" (a shift of hydrogen or deuterium to an adjacent position, implying a ketone intermediate) is in general agreement with the values obtained when the appropriate deuterated arene oxides are allowed to isomerize to phenols in solution at physiological pH.[3] For these reasons, it was initially thought that the mechanism of aromatic oxidation involved the insertion of an oxygen across the double bond, resulting in an arene oxide that would then isomerize to the phenol. However, evidence has been accumulating which suggests that nonarene oxide mechanisms may be involved in some cases. This evidence was first observed by Jerina et al. while investigating the metabolism of chlorobenzene.[4] The amount of meta hydroxy product formed was shown to be dependent on the enzyme preparation and generally higher than would be expected from the isomerization of arene oxides, which open almost exclusively to form ortho and para phenols. An even greater difference in product ratios was seen with the metabolism of 2,2',5,5'-tetrachlorobiphenyl in which more than 90% of the product was thought to proceed by a nonarene oxide mechanism.[5] Other evidence for an alternate pathway is provided by observed positive kinetic isotope effects during the formation of the meta hydroxy metabolites of methyl phenyl sulfone and nitrobenzene[6] and the formation of 7-hydroxywarfarin.[7]

The mechanistic alternative to the direct insertion pathway which has been supported in the recent literature is the addition–rearrangement mechanism shown in Scheme I. The initial step for this mechanism could be the addition of an oxygen which is "triplet-like", forming a radical or a biradical which can then rearrange to the phenol with or without going through an arene oxide intermediate. Alternatively, the initial step could be a one-electron oxidation of the substrate, giving a radical cation

Scheme I. Possible Addition-Rearrangement Mechanisms of Cytochrome P450 Mediated Oxidation of Aromatic Hydrocarbons

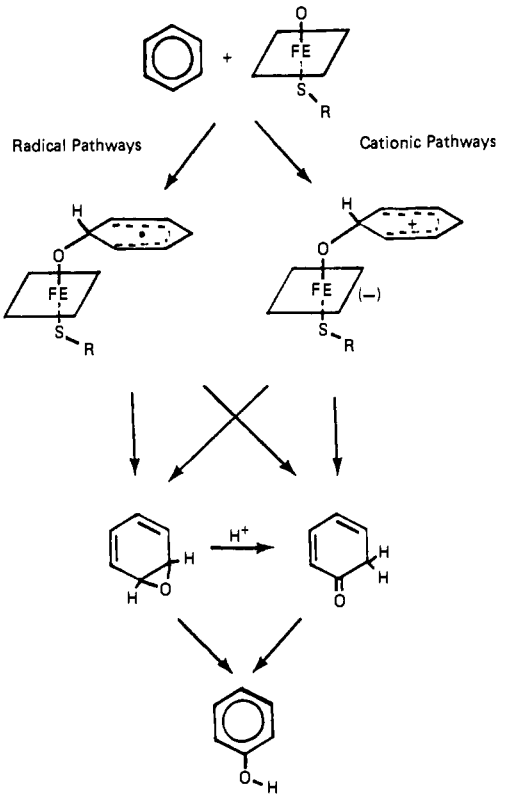

intermediate, which then combines with the oxygen. Evidence for such a one-electron oxidation has been seen in N-demethylation

[†]University of Washington.
[‡]SRI International.

(1) Jerina, D. M.; Daly, J. W.; Witkop, B.; Zaltzman-Nirenburg, D.; Udenfriend, S. *J. Am. Chem. Soc.* **1968**, *90*, 6525–6527.
(2) Jerina, D. M.; Daly, J. W.; Witkop, B.; Zaltzman-Nirenburg, D.; Udenfriend, S. *Biochemistry* **1970**, *9*, 147–155.
(3) Jerina, D. M.; Witkop, B. *Experentia* **1972**, *28*, 1129–1150.
(4) Selander, H. G.; Jerina, D. M.; Daly, J. W. *Arch. Biochem. Biophys.* **1983**, *158*, 309–321.
(5) Preston, B. D.; Miller, J. A.; Miller, E. C. *J. Biol. Chem.* **1983**, *258*, 8304–8310.
(6) Tamaszewski, J. E.; Jerina, D. M.; Daly, J. W. *Biochemistry* **1975**, *14*, 2024–2031.
(7) Bush, E. D.; Trager, W. F. *Biochem. Biophys. Res. Commun.* **1982**, *104*, 626–632.

0002-7863/85/1507-4273$01.50/0

Scheme II. Model Biradical Pathways Studied: Epoxide, Ketone, and Phenol Formation from Biradical Tetrahedral Intermediate

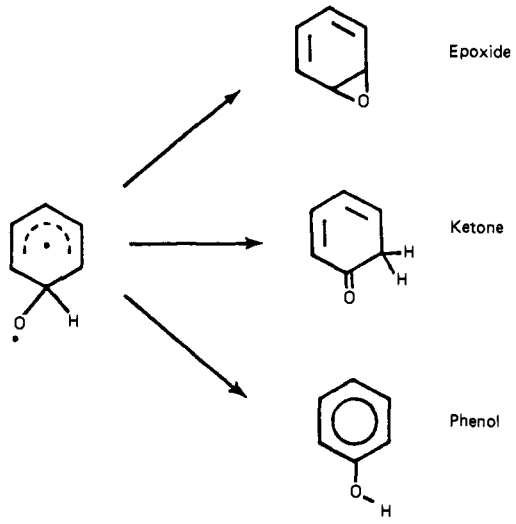

Scheme III. Model Cationic Pathways Studied: Epoxide, Ketone, and Phenol Formation from Closed-Shell (Nonradical) Cationic Tetrahedral Intermediate

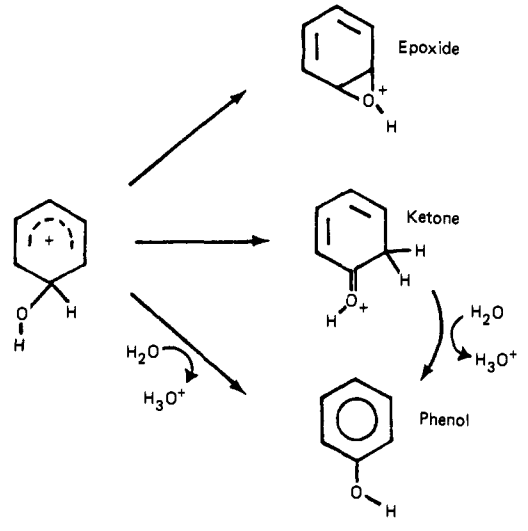

reactions,[8] reactions with cyclopropylamines,[9] dihydropyridine derivatives,[10] and the oxidation of halobenzenes.[11] After the electron abstraction, attachment of the substrate to the oxygen of the heme would result in a positive charge on the substrate ring. This state could also result from a charge transfer after or during the addition of the "triplet-like" oxygen on the substrate.

The work presented here describes an attempt to qualitatively evaluate both the radical and cationic pathways. To this end, the semiempirical quantum chemical method, MNDO, was used to characterize two model systems designed to represent the radical and cationic pathways of cytochrome P450 mediated aromatic hydrocarbon oxidations. Scheme II illustrates the biradical pathways studied, and Scheme III illustrates the model cationic pathways studied, each representing formation of epoxide, ketone, and phenol from a tetrahedral intermediate. For each of these pathways, enthalpies, and entropies of activation and reaction and kinetic isotope effects were calculated for a series of substituted chlorobenzenes and for naphthalene.

Table I. Calculated Properties for Biradical Tetrahedral Intermediates of Substituted Benzenes and Naphthalene

	(A) spin-paired (singlet) biradical			(B) triplet biradical		
X	ΔH_f[a]	S[b]	$\langle S^2\rangle$[c]	ΔH_f[a]	S[b]	$\langle S^2\rangle$[c]
H	33.7	76.2	1.5	32.1	77.6	2.5
4-CN	64.1	85.2	1.5	62.5	87.2	2.5
3-CN	65.3	85.2	1.5	63.7	87.2	2.6
4-OH	−15.8	82.3	1.5	−17.4		2.5
3-OH	−14.3	82.3	1.6	−15.9		2.6
4-Cl	26.2	*d*	1.5			
3-Cl	26.7		1.5			
2-Cl	26.7		1.5			
1-Cl	25.8		1.5			
naphthalene	42.2		2.0	40.7		3.1

[a] ΔH_f in kcal/mol. [b] S in cal/(mol·deg). [c] $\langle S^2\rangle$ eigenvalue of the spin operator; values >1 for spin-paired biradical and >2 for triplet biradical are caused by spin contamination (see Appendix). [d] When it became apparent that entropy effects were not important for the qualitative evaluation of the pathways, further values were not calculated.

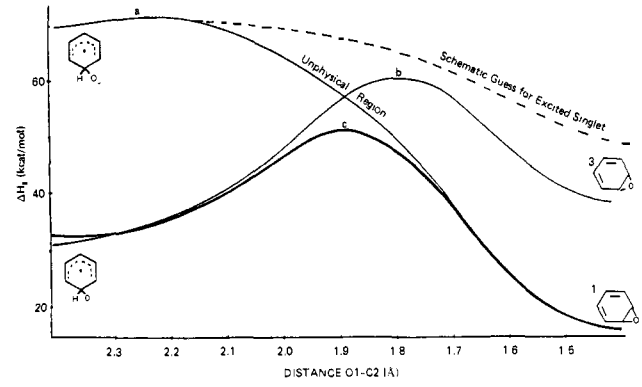

Figure 1. Reaction coordinates from tetrahedral intermediates to epoxides: (a) closed-shell singlet (Ψ_a), (b) triplet (Ψ_b), (c) open-shell singlet (Ψ_c). For the closed-shell singlet the dotted extension is more realistic than the "unphysical region". See Appendix.

Methods

The MNDO formalism[12,13] was used for all calculations, employing the unrestricted spin (UHF) method for treatment of open shells. Analytical derivatives were used for geometry optimizations and transition-state location with the final gradients less than 0.01 kcal/(mol. Å), and the final SCF energies coverged to 10^{-7} kcal or less. To search for transition states, one-dimensional reaction coordinates were chosen for the intramolecular rearrangement reactions and two-dimensional reaction coordinates for the bimolecular reactions. Minima and saddle points were verified by the occurrence of zero and one negative eigenvalue of the force constant matrix, respectively. Vibrational frequencies obtained from the mass weighted force constant matrix allowed calculation of the thermodynamic properties and the kinetic isotope effects as previously reported.[14]

Results

Biradical Pathways (Scheme II). Previous calculations[15] using triplet oxygen as a model for the initial attack by P450 on an aromatic system resulted in a biradical intermediate with one unpaired electron on the oxygen, the other on the ring, and the oxygen bound to the carbon atom in a tetrahedral manner. This biradical tetrahedral intermediate can exist in one of two spin states: the triplet state, in which the spins are unpaired, and the open-shell singlet state, in which the spins are paired. The calculated geometries (Figure 2a) and thermodynamic properties

(8) Shea, J. P.; Nelson, S. D.; Ford, G. P. *J. Am. Chem. Soc.* **1983**, *105*, 5451–5454.
(9) Hanzlik, P.; Tullman, R. H. *J. Am. Chem. Soc.* **1982**, *104*, 2048–2050.
(10) Augusto, O.; Beilan, H. S.; Ortiz de Montellano, P. R. *J. Biol. Chem.* **1982**, *257*, 11288–11295.
(11) Macdonald, B. L.; Zirvi, K.; Burka, L. T.; Peyman, P.; Guengerich, F. P. *J. Am. Chem. Soc.* **1982**, *104*, 2050–2052.
(12) Dewar, M. J. S.; Thiel, W. J. *J. Am. Chem. Soc.* **1977**, *99*, 4907–4919.
(13) Dewar, M. J. S.; Thiel, W. J. *J. Am. Chem. Soc.* **1977**, *99*, 4899–4907.
(14) Brown, B. S.; Dewar, M. J. S.; Ford, G. P.; Nelson, D. J.; Rzepa, H. S. *J. Am. Chem. Soc.* **1978**, *100*, 7832–7836.
(15) Pudzianowski, A. T.; Loew, G. H. *Int. J. Quantum. Chem.* **1983**, *23*, 1257–1268.

Table II. Epoxide Formation from a Singlet Biradical Tetrahedral Intermediate: Calculated Transition-State Properties, Enthalpies of Activation ($\Delta H^{\ddagger}$) and Reaction (ΔH_r) and Kinetic Isotope Effects (k_H/k_D)

	transition-state properties			activation and reaction properties		
X	ΔH_f[a]	S[b]	$\langle S^2\rangle$[c]	$\Delta H^{\ddagger}$[d]	ΔH_r[e]	k_H/k_D[f]
H	45.4	73.8	1.3	11.7	−17.8	0.9
4-CN	76.5	82.8	1.3	12.4	−16.4	0.9
3-CN	77.2	82.7	1.3	11.9	−18.3	
5-CN	77.1	82.8	1.3	11.8	−18.3	
4-OH	−3.9	79.6	1.3	12.0	−16.3	0.9
3-OH	−3.1		1.4	11.2	−17.7	
5-OH	−2.3		1.4	12.0		
4-Cl	33.4		1.3	12.2	−17.0	
3-Cl	38.8		1.3	12.1	−17.6	
2-Cl	40.7		1.3	14.0		
1-Cl	37.7		1.2	11.9		
naphthalene	52.6		1.8	10.4	−15.9	

[a] ΔH_f (kcal/mol) = enthalpy of formation of the transition state. [b] S (cal/(mol·deg)) = entropy of the transition state. [c] $\langle S^2\rangle$ = expectation value of the spin operator; values greater than one are an indication of "spin contamination" of singlet biradical species. [d] $\Delta H^{\ddagger}$ = enthalpy of activation in kcal/mol. [e] ΔH_r = enthalpy of reaction in kcal/mol. [f] k_H/k_D = calculated kinetic isotope effect, ratio of calculated rate constants without and with a deuterium at position C_2.

Table III. Epoxide Formation from Tetrahedral Intermediate on a Triplet Surface: Calculated Transition-State Properties, Enthalpies of Activation ($\Delta H^{\ddagger}$) and Reaction (ΔH_r), and Kinetic Isotope Effects (k_H/k_D).

	transition-state properties			activation and reaction properties		
X	ΔH_f[a]	S[b]	$\langle S^2\rangle$[c]	$\Delta H^{\ddagger}$[d]	ΔH_r[e]	k_H/k_D[f]
H	61.4	76.7	2.4	29.2	+5.9	0.9
4-CN	91.2	85.8	2.4	28.7	+5.6	0.9
3-CN	91.2		2.5	28.5		
5-CN	93.3	85.7	2.4	29.6		
4-OH	10.8		2.5	28.2	+4.6	
3-OH	9.4		2.4	25.3	+0.3	
5-OH	13.5		2.4	29.4		

[a] ΔH_f (kcal/mol) = enthalpy of formation of the transition state. [b] S (cal/(mol·deg)) = entropy of the transition state. [c] $\langle S^2\rangle$ = expection value of the spin operator; values greater than one are an indication of "spin contamination" of singlet biradical species. [d] $\Delta H^{\ddagger}$ = enthalpy of activation in kcal/mol. [e] ΔH_r = enthalpy of reaction in kcal/mol. [f] k_H/k_D = calculated kinetic isotope effect, ratio of calcualted rate constants without and with a deuterium at position C_2.

(Table I) for the triplet and singlet intermediates are almost identical. However, as shown in Figure 1, the reaction potentials are quite different. Figure 1 shows the reaction coordinates for epoxide formation from (a) the closed-shell singlet, (b) the triplet, and (c) the open-shell singlet, tetrahedral intermediates (see Appendix). While the triplet biradical remains on the triplet surface resulting in an excited epoxide, the singlet biradical mixes with the closed-shell surface, giving the ground-state epoxide. As a result of this mixing, the enthalpies of activation for epoxide formation from all substituted benzenes studied on the singlet surfaces are about 15 kcal lower than on triplet surfaces (Tables II and III) and are not very sensitive to substituent. The kinetic isotope effects (KIE) given are secondary KIEs since they are calculated for deuterium substitution at the C_2 position.

The transition-state geometry for the biradical singlet pathway to the epoxide is given in Figure 2b for unsubstituted benzene and is very similar for all analogues studied. As seen in this figure, an asymmetric 3-membered transition state is found with the oxygen still more closely bound to C_1 than to C_2 and with a mass weighted displacement vector indicating further movement toward C_2 to form the epoxide product.

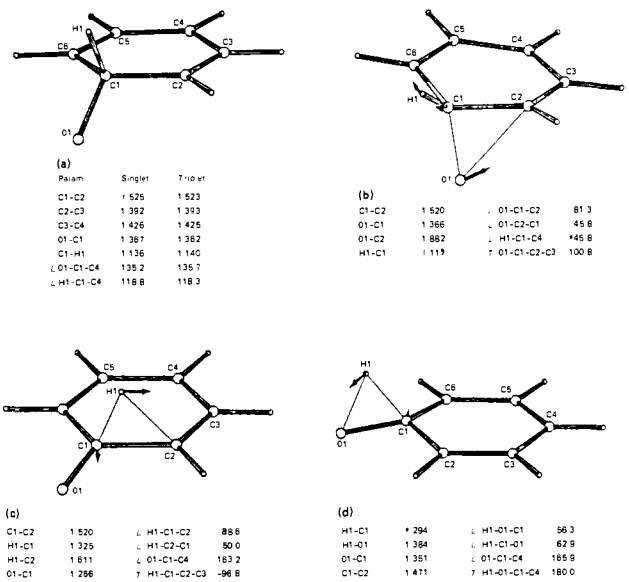

Figure 2. Biradical geometries: (a) tetrahedral intermediate, (b) transition state to epoxide, (c) transition state to ketone, (d) transition state to phenol.

Table IV. Ketone Formation from Singlet Biradical Tetrahedral Intermediate via 1,2-H Shift: Calculated Transition-State Properties; Enthalpies of Activation ($\Delta H^{\ddagger}$) and Reaction (ΔH_r), and Kinetic Isotope Effects (k_H/k_D)

	transition-state properties			activation and reaction properties		
X =	ΔH_f[a]	S[b]	$\langle S^2\rangle$[b]	$\Delta H^{\ddagger}$[d]	ΔH_r[e]	k_H/k_D[f]
H	57.5	74.9	1.2	23.8	−45.7	4.6
3-CN	89.8		1.3	24.4	−45.2	
4-OH	8.4		1.2	24.2	−43.6	
3-OH	9.5		1.3	23.8	−46.4	
naphthalene	65.9		1.8	23.7	−43.2	

[a] ΔH_f (kcal/mol) = enthalpy of formation of the transition state. [b] S (cal/(mol·deg)) = entropy of the transition state. [c] $\langle S^2\rangle$ = expectation value of the spin operator; values greater than one are an indication of "spin contamination" of singlet biradical species. [d] $\Delta H^{\ddagger}$ = enthalpy of activation in kcal/mol. [e] ΔH_r = enthalpy of reaction in kcal/mol. [f] k_H/k_D = calculated kinetic isotope effect, ratio of calculated rate constants without and with a deuterium substitution for H_1 (hydrogen that is transferred from C_1 to C_2).

The results obtained here favor a singlet biradical pathway over a triplet pathway to epoxide formation from the tetrahedral intermediate. In the P450 mediated enzymatic process, the tetrahedral intermediate will probably be bound to the heme and, even if it has some unpaired spin density initially, the iron would facilitate a triplet-to-singlet crossover. For these reasons, only the singlet biradical pathways were considered for the remaining biradical calculations.

Figure 2c and Table IV summarize the results obtained for formation of a ketone directly from a singlet birdical intermediate via a 1,2-hydrogen shift. As shown in Figure 2c, the transition state found is characterized by a partial shift of the H (H_1) from C_1 to C_2 ($r(H_1–C_1)$ = 1.325 Å, $r(H_1–C_2)$ = 1.61 Å) forming a 3-membered ring. The mass weighted displacement vector of the vibrational mode corresponding to the reaction coordinate indicates the continuing shift of this hydrogen to the adjacent carbon (C_2) to form the ketone.

As seen in Table IV, for each of the five analogues studied, the enthalpies of activation for ketone formation (Figure 2c) are about 12 kcal/mol higher than those for epoxide formation (Table II) and again are not significantly affected by the substituents on the aromatic ring nor in going from benzene to naphthalene.

Figure 2d and Table V summarize the results obtained for direct phenol formation from the biradical intermediate by rearrange-

Table V. Calculated Properties for Singlet Biradical Tetrahedral Intermediate Rearrangement to Phenols

	transition-state properties			activation and reaction properties		
X	ΔH_f[a]	S[b]	$\langle S^2\rangle$[c]	$\Delta H^{\ddagger}$[d]	ΔH_r[e]	k_H/k_D[f]
H	64.3	75.3	1.3	30.5	−60.5	3.7
3-CN	95.7		1.4	30.4	−60.9	
3-OH	15.9		1.4	30.3	−60.5	

[a] ΔH_f (kcal/mol) = enthalpy of formation of the transition state. [b] S (cal/(mol·deg)) = entropy of the transition state. [c] $\langle S^2\rangle$ = expection value of the spin operator; values greater than one are an indication of "spin contamination" of singlet biradical species. [d] $\Delta H^{\ddagger}$ = enthalpy of activation in kcal/mol. [e] ΔH_r = enthalpy of reaction in kcal/mol. [f] k_H/k_D = calculated kinetic isotope effect, ratio of calculated rate constants without and with a deuterium substitution for H_1 (hydrogen that is transferred from C_1 to O).

Table VI. Calculated Thermodynamic Properties for the Protonated Cationic Tetrahedral Intermediate of Substituted Benzenes and Naphthalene

X	ΔH_f, kcal/mol	S, cal/(mol·deg)	X	ΔH_f, kcal/mol	S, cal/(mol·deg)
H	172.8	79.1	$4OCH_3$	117.4	
			$3OCH_3$	135.7	
4-CN	213.5	87.7			
3-CN	212.9		4F	128.5	
2-CN	213.1				
4-OH	111.8	83.9	$4CH_3$	162.3	
3-OH	129.9	84.8	$3CH_3$	164.6	
2-OH	111.0		naphth	176.1	91.7
4-Cl	170.9	86.1			
3-Cl	172.7	85.6			
2-Cl	171.2				

ment of the H from C_1 to the oxygen atom. As shown in Figure 2d, the transition state found is characterized by partial transfer of the H from C_1 to O_1, forming an asymmetric 3-membered ring. Again, the mass weighted displacement vector of the vibrational mode corresponding to the reaction coordinate indicates further movement of H_1 toward O_1 to form the phenol product.

As seen in Table V for the three analogues studied, direct phenol formation has an enthalpy of activation ~18 kcal/mol higher than that for corresponding epoxide formation (Table II) and ~7 kcal/mol higher than that for ketone formation (Table IV) and no substituent effect.

The kinetic isotope effects given for ketone and phenol formation in Table IV and V are primary isotope effects calculated by deuterium substitution at C_1, the hydrogen being transferred from the tetrahedral carbon C_1 to C_2 to form the ketone or to the oxygen to form the phenol.

Cationic Pathways. As shown in Scheme III, the starting point for the cationic pathway modeled was the protonated closed-shell tetrahedral intermediate, which has a positive charge on the ring. The optimized geometry of the unsubstituted benzene intermediate is given in Figure 3a, and the calculated enthalpies of formation and entropies of all protonated intermediates are given in Table VI. In contrast to the biradical intermediate (Table I), the results shown in this table indicte significant substituent effects, especially among the isomers of hydroxy- and methoxy-substituted benzene intermediates. The para-substituted compounds have heats of formation ~18 kcal lower than their meta isomers.

The geometry of the transition state to the protonated epoxide for the unsubstituted benzene is given in Figure 3b. This result is typical of all the transition states obtained for the substituted benzenes. As seen in Figure 3b, this transition state greatly resembles that for the biradical pathway to epoxide formation. Again an asymmetric 3-membered ring is formed, indicating partial attachment of the oxygen to C_2. However, oxygen attachment to C_2 is somewhat more advanced in the cationic transition state (Figure 3b) than in the corresponding biradical transition state (Figure 2b). The enthalpies and entropies for the

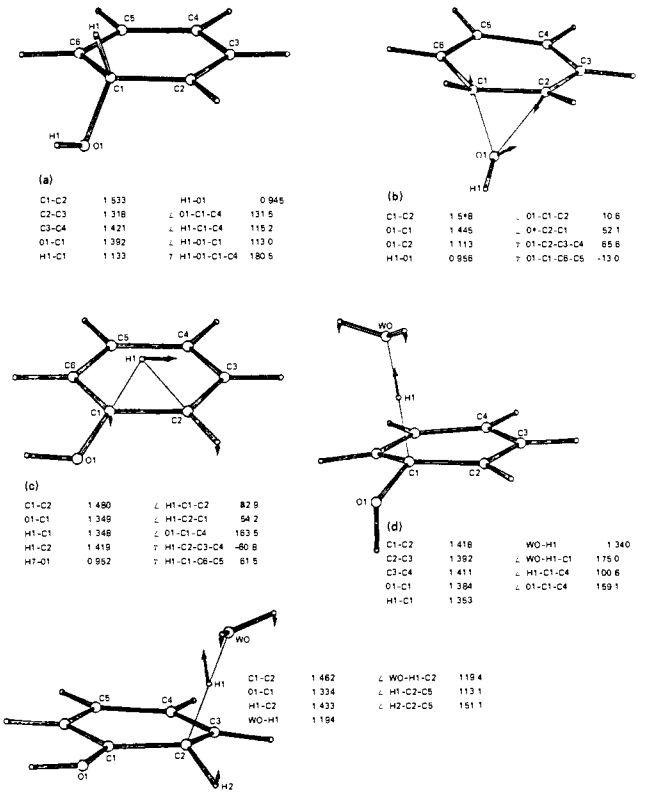

Figure 3. Protonated cationic geometries: (a) tetrahedral intermediate, (b) transition state to epoxide, (c) transition state to ketone, (d) transition state to phenol, (e) transition state from ketone to phenol.

Table VII. Protonated Epoxide Formation from Cationic Tetrahedral Intermediates: Calculated Transition-State Enthalpies and Entropies of Activation

	transition-state properties		activation enthalpy
X	ΔH_f, kcal/mol	S, cal/(mol·deg)	$\Delta H^{\ddagger}$, kcal/mol
H	200.1	73.4	27.2
4-CN	239.9	82.1	26.3
3-CN	238.7		25.8
5-CN	239.2		26.3
4-OH	146.9	80.0	35.1
3-OH	150.9	78.5	21.0
5-OH	154.4		24.4
4-Cl	198.4		27.5
3-Cl	199.1		26.3
5-Cl	198.8		26.1

transition states shown in Figure 3b and the corresponding enthalpies of activation for formation of the protonated epoxides are summarized in Table VII for all the substituted benzenes studied. Loss of a proton from this species was assumed to be rapid compared to ring closing and was not modeled.

The geometry of the transition state to the protonated ketone via a 1,2-hydrogen shift from the cationic tetrahedral intermediate is given in Figure 3c for unsubstituted benzene. This transition state is similar for all substituted benzenes and resembles that for the biradical pathway to ketone formation (Figure 2c) with transfer of the hydrogen to C_2 somewhat more complete. The enthalpies and entropies of these transition states for all the substituted benzenes characterized are given in Table VIII together with corresponding calculated enthalpies of activation for formation of protonated ketones. Loss of a proton from this species was assumed to be rapid compared to the 1,2-H shift and was not modeled.

Direct phenol formation from the cationic tetrahedral intermediate involves loss of a proton from C_1 which then is the

Table VIII. Protonated Ketone Formation from Cationic Tetrahedral Intermediates: Calculated Transition-State Enthalpies and Entropies of Activation

X	transition-state properties		activation enthalpy
	ΔH_f, kcal/mol	S, cal/(mol·deg)	$\Delta H^{\ddagger}$, kcal/mol
H	195.1	75.0	22.2
4-CN	235.1	83.7	21.5
3-CN	234.8		21.9
5-CN	235.2		22.2
4-OH	143.2	79.9	31.4
3-OH	150.3	80.9	20.4
5-OH	147.3		17.4
4-Cl	193.9	82.1	23.0
3-Cl	194.6		21.8
5-Cl	194.3		21.6
naphthalene	203.9	88.4	27.8

Table IX. Water-Assisted Direct Phenol Formation from Cationic Tetrahedral Intermediates: Calculated Transition-State Enthalpies and Entropies of Activation

X	transition-state properties		activation enthalpy
	ΔH_f, kcal/mol	S, cal/(mol·deg)	$\Delta H^{\ddagger}$, kcal/mol
H	129.2	89.1	17.3
4-CN			
3-CN	167.6	97.9	15.6
4-OH	74.4	93.5	23.6
3-OH	84.1	95.1	15.1
4-Cl	127.1	96.1	17.2
3-Cl	127.6	96.3	15.8
4-CH_3	120.1		18.8
3-CH_3	121.4		17.4
naphthalene	140.7	101.1	35.3

rate-determining step. To model the pathway to direct phenol formation a neutral water molecule was used to abstract the proton (H_1) at the tetrahedral carbon (C_1). The transition state obtained is shown in Figure 3d. In this transition state the proton is shared nearly equally between the tetrahedral carbon and the water oxygen ($r(C_1-H_1)$ = 1.353 Å, $r(WO-H_1)$ = 1.34 Å). The displacement vector of the reaction coordinate indicates further H abstraction to form the phenol product. The thermodynamics and the calculated enthalpies of activation for this reaction for a series of substituted benzenes are given in Table IX.

Comparisons of the calculated enthalpies of activation given in Table IX for the phenol with those in Table VIII for the ketone and in Table VII for the epoxide indicate that the barrier to the water-assisted pathway to phenol formation is ~5 kcal/mol lower than that for protonated ketone formation which in turn is ~5 kcal/mol lower than for formation of epoxides; and all are sensitive to substituents.

In addition to direct phenol formation by loss of a proton from C_1 of the cationic tetrahedral intermediate, phenol formation can also occur by enolization of the protonated ketone. As shown in Scheme III, this process corresponds to loss of a proton from C_2 of the ketone. This is also the enolization reaction presumed to occur in the solvent during the acid-catalyzed rearrangement of the epoxide. The water-assisted removal of this proton was therefore modeled, and the transition state obtained is shown in Figure 3e. This transition state is very similar to that for direct phenol formation (Figure 3d) but with transfer of the proton to the H_2O more complete ($r(C_2-H_1)$ = 1.34 Å, $r(WO-H_1)$ = 1.19 Å). Only the H, 3-CN, and 4-OH compounds were modeled, giving enthalpies of activation and primary KIEs summarized in Table X. Comparing these results with those given in Table IX, we see that for each analogue, H_2O-assisted enolization has a 3 to 7 kcal/mol higher enthalpy of activation than the corresponding water-assisted direct formation of phenols (Table IX). However, enolization of a protonated ketone has a much lower barrier than enolization of an unprotonated ketone by direct transfer of a hydrogen on C_2 to the unprotonated ketone oxygen. This latter reaction was modeled on a closed-shell singlet surface for unsubstituted benzene and found to have an enthalpy of activation of 90 kcal/mol, compared to 24.8 kcal/mol for the acid-catalyzed, solvent-assisted pathway (Table X).

Table X. Water-Assisted Enolization of Protonated Ketones

X	activation enthalpy $\Delta H^{\ddagger}$, kcal/mol	kinetic isotope effect k_H/k_D (D at C_2)
H	24.8	5.9
3-CN	23.0	6.0
4-OH	20.9	

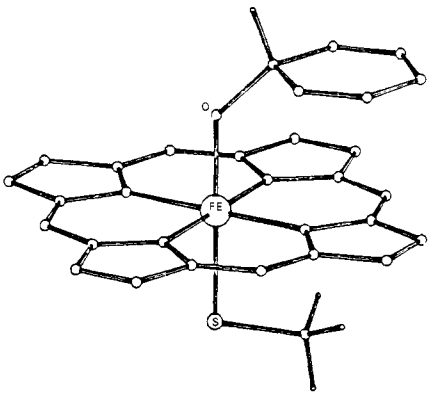

Figure 4. Model ferryl P450–substrate complexes used in preliminary studies.

Discussion

There is an increasing amount of evidence that cytochrome P450 mediated aromatic hydroxylation occurs by radical addition, but with the additional possibility of electron transfer from the substrate to the heme unit which can result in an intermediate with a positive charge on the aromatic ring of the substrate (see Scheme I). Preliminary calculations,[16] using an INDO method parameterized for transition metals,[17] have been made in our laboratory for model ferryl cytochrome P450–substrate complexes shown in Figure 4, with benzene and phenol. The results suggest that the extent of charge transfer and spin density on the substrate resulting in either a radical or cationic species may be substituent dependent, with electron-donating groups favoring the cationic species.

The simplified, non-heme model we have used in reaction pathway studies to represent these biradical and cationic forms of the tetrahedral intermediate in order to characterize pathways to product formation from it cannot address the question of which form will be preferred for a given substituted benzene substrate in the environment of the heme unit in the protein. However, the results do allow us to examine the consequences of each type of mechanism.

The results obtained here strongly suggest that if product formation occurs via a birdical pathway, aryl ring carbon oxidations by cytochrome P450 proceed through an epoxide intermediate. By contrast, if there is an electron transfer from the substrate when it forms a tetrahedral addition complex with the electrophilic oxygen still bound to the heme group, or if the tetrahedral complex becomes protonated at the heme substrate binding site after dissociation from the heme, then direct phenol formation is favored over either ketone or epoxide formation.

(16) Unpublished results obtained in our laboratory. UHF results contain a large amount of spin contamination.

(17) Zerner, M. C.; Loew, G. H.; Kirchner, R. F.; Muller-Westerhoff, U. T. *J. Am. Chem. Soc.* **1980**, *102*, 589–599.

Moreover, the cationic pathway is sensitive to substituent effects, while the biradical pathway is not.

For the biradical pathways, epoxide formation appears to be greatly favored over ketone or phenol formation, with enthalpies of activation of 12, 24, and 30 kcal/mol, respectively. The effects of entropy on these reactions appear to be negligible, with $T\Delta S$ less than 1 kcal/mol. The substituent effects on the pathways are minimal, and the isotope effects are as expected: positive for ketone and phenol formation, where a hydrogen or deuterium atom is being transferred, and inverse for epoxide formation with an adjacent deuterium, due to a change from sp^2 to sp^3 hybridization.

The biradical pathways will probably be least susceptible to environmental effects, since charge stabilization is not necessary. However, there are three major deficiencies in the calculations which should be considered in evaluating the results obtained. First, the unrestricted Hartree–Fock (UHF) method was used for the SCF calculations, a method which can result in an overestimation of the correlation energy[18] due to "spin contamination" (values of $\langle S^2 \rangle > 1$) and thus a calculated heat of formation which is too low. While errors in the energy due to this contamination cannot be evaluated, it is encouraging that changes in $\langle S^2 \rangle$ from tetrahedral intermediates to transition states remain essentially the same for epoxide and ketone formation (i.e., 0.22 to 0.27 and 0.26 to 0.28, respectively) and are only somewhat higher ($\sim$0.1) for the phenols. Therefore, spin contamination may not be a problem when comparing the relative value of enthalpies of activation for different pathways.

Another, more difficult, problem results from the general tendency of MNDO to overestimate activation enthalpies,[14,15,19] especially those in which hydrogen atoms are transferred. The transition state to the ketone may therefore be overestimated relative to the epoxide pathway. However, extensive ab initio calculations (MCSCF, double-ζ, with polarization functions) have been previously done on a similar system—the biradical resulting from the addition of triplet oxygen to ethylene.[20] These calculations gave a 10.3-kcal/mol energy of activation for the hydrogen shift pathway (resulting in an aldehyde) and a very small barrier to epoxide formation.[21] MNDO calculations we have performed on the same system gave a 22-kcal/mol barrier for ketone formation and a 7-kcal/mol barrier for epoxide formation (data not shown). Thus the order and relative difference are in fairly good agreement with the values calculated for the aromatic system and are consistent with the ab initio calculations.

The third important problem with the simplified biradical model is the absence of any explicit electronic or steric effects of the heme system. If the tetrahedral intermediate is bound to the heme, there is no guarantee that electronic effects will cancel for the different pathways leadings to epoxide, ketone, and phenol. Also, steric factors, especially from the heme, may be different for these different pathways.

Nevertheless, given all these considerations, with the epoxide pathways about 12 kcal/mol lower than the ketone pathway, the sum of the above deficiencies would have to be great to change the qualitative conclusion that the epoxide pathway is favored over both ketone and direct phenol formation for a radical mechanism. Thus if the biradical pathway were the only one possible, our results strongly suggest that phenol formation would occur primarily via an epoxide intermediate.

For the cationic pathway, an entirely different qualitative picture emerges. Direct phenol formation is competitive with both epoxide formation and formation of phenols via a ketone intermediate. Moreover, the extent to which these "direct" and indirect pathways to phenol formation occur are substituent dependent. The numerical results obtained in each case favor direct phenol formation and hence do not predict deuterium retention seen when either epoxides or ketones rearrange to phenols. The barrier to the water-assisted pathway to phenol formation is 10 to 12 kcal/mol lower than that to expoxide and 5 to 7 kcal/mol lower than that to ketone formation, and this would result in almost no deuterium retention. However, ketones, phenols, and epoxides and the transition states obtained for their formation from the cationic tetrahedral intermediate are very different, and differences in charge stabilization, interactions of the solvent with the transition state, and entropy effects could easily cause a reversal in the preferred pathway.

The model system chosen for the cationic pathways has the advantage that the proton on the oxygen at least mimics the Lewis acidity of the heme. However, it has the disadvantage of having a more localized positive charge, relative to that which would exist in the heme. Experimentally, it has been shown[22] that the rearrangement of epoxides to phenols is acid catalyzed, with initial ring opening of epoxides leading to the same cationic tetrahedral intermediate used to model the P450 modulated cationic pathways. Care must be taken, however, to differentiate between the three systems involved: acid-catalyzed rearrangements of epoxides in solution, the conditions at the active site of cytochrome P450, and the gas-phase systems used to model them in these calculations. It would perhaps be more reasonable to compare the effect of different substituents on the activation enthalpies within each pathway, comparisons in which some of the deficiencies may cancel.

The amount of deuterium retention as a function of substituent variation does seem to follow the trend observed in the calculated enthalpies of activation for the water-assisted pathway to phenol formation (shown in Table IX). For example, Hanzlik et al.[23] have found that the formation of the 3- and 4-CN; the 3-methyl-, and the 3-methoxyphenols occurs with low deuterium retention. These are also the products which give the lowest enthalpies of activation in the series studied.

The maximum deuterium retention value reported is $\sim$80%, suggesting that the enolization of the ketone had a KIE of about 4. This is in general agreement with the calculated KIE of 6 for the ketone to phenol pathway (Table X) which gives a maximum theoretical retention value of 86%. The similar values of KIEs calculated for the 3-CN (low deuterium retention) and benzene (high deuterium retention) suggest that the differences in deuterium retention observed for phenol formation is not due to a difference in the enolization transition-state structure, but due to a difference in the contribution from a competing pathway such as the direct path from the tetrahedral intermediate to the phenol.

The active site of cytochrome P450 is thought to be lipophilic in nature, and the aromatic ring of a cationic substrate intermediate would certainly interact with the prophyrin ring of the heme forming a charge-transfer complex, unless prevented by steric factors. The net charges on the aromatic ring of substituted benzene in the transition states for epoxide and ketone formation are +0.23 and +0.24, respectively. Thus one may infer that charge stabilization for these pathways is similar and the ketone formation is favored over epoxide formation. The direct pathway to the phenol is also possible, provided that a basic group is available to abstract the hydrogen.

In summary, although no quantitative conclusions can be drawn, our results suggest that a radical mechanism of aryl oxidations would favor epoxide formation, and a cationic mechanism would favor direct phenol or ketone formation. Comparisons of experimental and theoretical results are most consistent with the conclusion that both pathways may be involved in cytochrome P450 oxidations of aromatic hydrocarbon substrates and would be modulated by the nature of substituents as well as the aromatic system itself.

Acknowledgment. Helpful discussions with Dr. George Ford and support for this work for G. Loew and D. Spangler from NIH Grant GM 27943 and for W. Trager and K. Korzekwa from NIH Grant 07750 are gratefully acknowledged.

(18) Dewar, M. J. S.; McKee, M. L. *Pure Appl. Chem.* **1980**, *52*, 1432.
(19) Pudzianowski, A. T.; Loew, G. H.; Mico, B. A.; Branchflower, R. V.; Pohl, L. R. *J. Am. Chem. Soc.* **1983**, *105*, 3434–3438.
(20) Lester, W. A.; Dupuis, M.; O'Donnell, T. J.; Olson, A. J. "Frontiers in Chemistry"; Pergamon Press: New York, 1982; pp 159–167.
(21) Dupuis, M., private communication.
(22) Bruice, T. C.; Bruice, P. Y. *Acc. Chem. Res.* **1976**, *9*, 378–383.
(23) Hanzlik, R. P.; Hogberg, K.; Judson, C. M. *Biochemistry*, in press.

Appendix

Spin Multiplicity and Potential Curves (Figure 1). The open-shell "triplet" states are specified as having $S_z = 1$ with no relation between the spin up and spin down orbitals. The open-shell "singlet" states are specified as having $S_z = 0$ and no relation between spin up and spin down orbitals. If we had a restricted open-shell triplet and singlet, the Slater determinants would be

$$\Psi_t = \langle \Phi_i \bar{\Phi}_i \ldots \Phi_{n-1} \bar{\Phi}_{n-1} \Phi_n \Phi_m \rangle \quad \text{(A-1)}$$

$$\Psi_s = \langle \Phi_i \bar{\Phi}_i \ldots \Phi_{n-1} \bar{\Phi}_{n-1} \Phi_n \bar{\Phi}_m \rangle \quad \text{(A-2)}$$

These states have $\langle S^2 \rangle$ and 2 and 1, respectively, since Ψ_t is a true triplet with $S_z = 1$ while Ψ_s is a 50–50 mixture of a true triplet with $S_z = 0$ and a true singlet. However, as shown in Table I, $\langle S^2 \rangle$ for the open-shell "singlet" (Ψ_c) and "triplet" (Ψ_b) states are respectively 1.5 and 2.5. The extra 0.5 above what is required for restricted states (A-1) and (A-2) presumably represents the contribution from a lack of complete identity of spin-paired electrons $\Phi_i \bar{\Phi}_i$ due to the different electron repulsion of the unpaired electrons Φ_n and Φ_m. While the true ground state should be a triplet, the calculated ground state picks up contributions from states of higher multiplicity in an attempt to minimize total energy with a singlet Slater determinantal wave function. In this way the state is modified to include some correlation energy.

For states Ψ_b and Ψ_c (curves b and c of Figure 1), the outer orbitals Φ_n and Φ_m are similar. Thus the energy gap between the states represents half the energy between the true singlet and triplet biradicals, since Ψ_c is necessarily a 50–50 mixture of these. Presumably when the triplet oxygen atom is transferred to benzene, the intial state formed is the triplet. The presence of the neighboring porphyrin ring with unpaired electrons should cause fast relaxation among the three triplet and one singlet states of curves b and c. However, only from the singlet state will the molecules cross over to form the epoxide product. If the relaxation among the singlet and triplet states is fast compared to the rate of crossing the potential barrier, the effect of spin would be to reduce the rate to $^1/_4$ its value for the singlet alone.

The "potential curve" for the closed-shell singlet, Ψ_a in Figure 1, does not represent any real curve since our calculational method does not require that Ψ_a and Ψ_c be orthogonal. The merger of the a and c potential curves is an artifact of our calculational method and represents the region where the ground state becomes closed shell in character. The true second singlet state should occur at energies above the lowest triplet state—at least at the right end of the diagram where we are dealing with the closed-shell epoxide product. We have indicated on Figure 1 a qualitative guess for the unphysical region of curve a and the form of the true second singlet curve.

The MNDO method has been parameterized to give good ΔH_f for closed-shell molecules. Our potential curves (Figure 1) carry us from an open-shell biradical to a closed-shell product. It is not clear, at this time, whether this method introduces systematic errors along this curve.

Crystal Structure of Aspartame, a Peptide Sweetener

Marcos Hatada,† Jarmila Jancarik, Bradford Graves, and Sung-Hou Kim*

Contribution from the Department of Chemistry and Lawrence Berkeley Laboratory, University of California, Berkeley, California 94720. *Received October 25, 1984*

Abstract: We report on the crystal structure of aspartame, a dipeptide having an intensely sweet taste. The molecule has a molecular formula $C_{14}N_2O_5H_{18}\cdot{}^1/_2H_2O$ and crystallizes in space group $P4_1$ with cell parameters $a = b = 17.685$ (5) Å, and $c = 4.919(2)$ Å, $z = 4$. The final R value is 4.5%. The structure reveals an interesting arrangement of molecules in the crystal, which explains its solution behavior and may be important in designing new and modified sweeteners that will help further our understanding of the structural basis for sweet taste.

Aspartame is a new type of sweetener, about 200 times sweeter than sugar, and is currently widely used as a sugar substitute in beverages and low-calorie foods. The molecule is a methyl ester of the dipeptide L-aspartyl-L-phenylalanine[1] and is sold under the brand name of "NutraSweet" by G. D. Searle and Co. of Skokie, IL.

The molecule in aqueous solution is heat labile and pH sensitive; at 25 °C the optimum pH is 4.2, with a half-life of 260 days, but at higher temperature and pH, the molecule loses its sweet taste and degrades very rapidly to aspartylphenylalanine or its diketopiperazine, then to aspartic acid and phenylalanine. Aspartame is slightly soluble in water (about 5% at 20 °C and pH 7) and sparingly soluble in alcohol. It has a strong tendency to form very fine fibres when crystallized.

Substitution of other amino acids for aspartic acid and phenylalanine showed that aspartic acid is essential for the sweet taste. Furthermore, of the four possible diastereoisomers of aspartame, only the LL isomer was sweet.[2,3]

Though theories on sweet taste are not highly developed, considerable efforts have been directed toward chemical modification of aspartame and designing new aspartic acid based sweeteners.[3] Examination of many sweet compounds suggests that most of them have an electronegative atom B and a polarized hydrogen donor system A–H with a distance between A and B of about 3 Å[4] and a third and hydrophobic group X at distances of 3.5 and 5.5 Å from A and B, respectively.[5] In aspartame, the A–H:B system is present at the aspartyl residue where $-NH_3^+$ represents A–H and the oxygens of the aspartate sidechain represent B. But there is no candidate for the X group.

Experimental Section

As mentioned earlier, aspartame crystallizes out from most common aqueous and organic solvents as extremely fine fibres, unsuitable for X-ray crystallographic studies. After screening a large number of binary and ternary solvent systems, a suitable aspartame crystal was obtained from a quaternary solvent system: the sample was dissolved to super-

†Present address: Department of Chemistry, University of California—San Diego, La Jolla, CA 92093.

(1) Mazur, R. H.; Schlatter, J. M.; Goldkamp, A. H. *J. Am. Chem. Soc.* **1969**, *91*, 2684.
(2) Mazur, R. H. Symposium: "Sweeteners"; Inglett G. E., Ed.; Avi Publishing Co.: Westport, CT, 1974; p 159.
(3) Mazur, R. H.; Goldkamp, A. H.; James, P. A.; Schlatter, J. M. *J. Med. Chem.* **1970**, *13*, 1217.
(4) Shallenberger, R. S.; Acree, T. E. *Nature (London)* **1967**, *216*, 480.
(5) Kier, L. B. *J. Pharm. Sci.* **1972**, *61*, 1394.

0002-7863/85/1507-4279$01.50/0